^{17}O Hyperfine Structure of the Neutral ($S=1$) Vacancy-Oxygen Center in Ion-Implanted Silicon†

K. L. Brower
Sandia Laboratories, Albuquerque, New Mexico 87115
(Received 27 December 1971)

The intensity of the ^{17}O hyperfine spectrum associated with the ^{28}Si-^{17}O-^{28}Si isotopic configuration of the vacancy-oxygen (Si-$S1$) center was enhanced by ion implantation of ^{17}O into silicon. The Si-$S1$ ^{17}O hyperfine spectrum was measured by electron paramagnetic resonance. An analysis of the Si-$S1$ ^{17}O hyperfine spectrum indicates that the numerical values for the elements in the ^{17}O hyperfine coupling tensor $\overleftrightarrow{A}$ are $A_{xx}=-11.5_1\times10^{-4}$ cm^{-1}, $A_{yy}=-12.9_0\times10^{-4}$ cm^{-1}, and $A_{zz}=-13.3_9\times10^{-4}$ cm^{-1}. The ^{17}O hyperfine coupling tensor was analyzed in terms of the admixture of oxygen-valence orbitals into the one-electron paramagnetic molecular orbitals $\chi_1(\Gamma_1)$ and $\chi_4(\Gamma_4)$. In particular, only 4.1% of $\langle\chi_1(\Gamma_1)|\chi_1(\Gamma_1)\rangle$ and 1.8% of $\langle\chi_4(\Gamma_4)|\chi_4(\Gamma_4)\rangle$ are localized on the oxygen atom in this defect.

I. INTRODUCTION

The Si-$S1$ center has previously been identified as the neutral charge state of the vacancy-oxygen center in silicon in an excited triplet spin state.[1] It is the negative charge state of this defect which gives rise to the Si-$B1$ spectrum.[1-4] The molecularlike structure of this defect is illustrated in Fig. 1. The vacancy-oxygen center can be formed in silicon which contains oxygen as an impurity by irradiation with electrons, neutrons, or ions.

In electron paramagnetic resonance (EPR) studies dealing with the electronic and molecular structure of defects, the hyperfine interactions play a very important role. Besides being able to identify specific isotopes and imposing certain constraints on the position of these isotopes in a defect, the hyperfine interaction is analogous to a projection operator which extracts from the paramagnetic molecular orbitals the admixture of s- and p-like orbitals localized on each site from which a resolved hyperfine spectrum originates. So far, the coupling tensors in the spin Hamiltonian which describe the Si-$S1$ fine-structure and

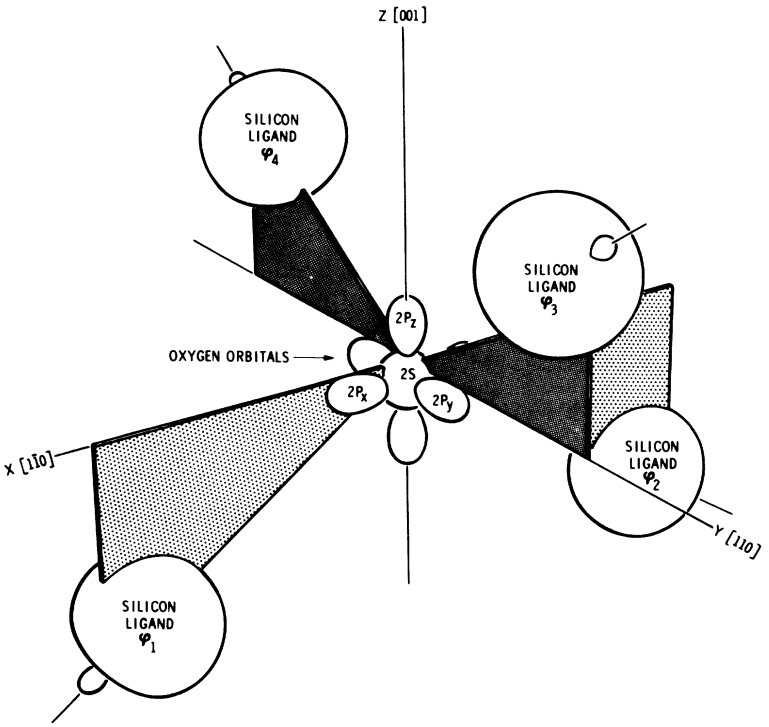

FIG. 1. Structure of the vacancy-oxygen center in silicon. In this schematic, the oxygen atom is displaced along the z axis from the tetrahedral site (origin of XYZ). This distortion lowers the symmetry of the defect from T_d to C_{2v}. The allowed linear combinations of silicon ligands φ_i and oxygen orbitals for these symmetries are tabulated in Table III.

^{29}Si hyperfine interactions have been determined.[1] In particular, analyses of the ^{29}Si hyperfine coupling tensors have contributed information regarding the admixture of 3s and 3p silicon valence orbitals localized on various silicon sites neighboring the vacancy-oxygen complex.[1,4] The phenomenological description of the wave function deduced from the ^{29}Si hyperfine interactions does seem to describe the spatial extent of the paramagnetic electrons in the Si-$S1$ center reasonably well as evidenced by the agreement between the measured and calculated electronic spin-spin interaction.[1]

The objective of the experiment described in this paper was to determine the ^{17}O hyperfine coupling tensors and to deduce from the ^{17}O hyperfine interaction the admixture of 2s and 2p oxygen-valence orbitals in the molecular orbitals describing the paramagnetic electrons. The ^{17}O isotope is unique to this study because it is the only stable oxygen isotope with a nonzero nuclear spin ($I = \frac{5}{2}$). On the other hand, ^{17}O is only 0.037% naturally abundant so that the ^{17}O hyperfine spectrum is ordinarily very weak and unresolved from the fine-structure and ^{29}Si hyperfine spectra.[1] This difficulty has been overcome by implanting ^{17}O into silicon samples and thereby significantly enhancing the intensity of the ^{17}O hyperfine spectrum relative to the fine-structure spectrum.

II. EXPERIMENT

The implantation of various ions into the samples was achieved with an Accelerators Inc. machine. The ion source consisted of a plasma generated by rf excitation of an appropriate gas from which ions were extracted and accelerated. Since ^{17}O is only 0.037% naturally abundant, a 100-cm^3 ampule of oxygen gas enriched with 70% $^{16}O_2$, 10% $^{17}O_2$, and 20% $^{18}O_2$ was the source of oxygen for the ^{17}O implants. The desired ions were selected by means of an $\vec{E} \times \vec{B}$ velocity filter. Usually the samples were implanted with 180-keV $^{17}O^+$ ions.

The Si-$S1$ spectrum observed by EPR in silicon implanted with ^{17}O is shown in Fig. 2. Because the ^{17}O hyperfine and the nuclear Zeeman interactions lift the sixfold degeneracy of the ^{17}O nuclear-spin states, the ^{17}O hyperfine spectrum is characterized by six nearly evenly spaced resonances. Since the tail of the $^{16}O^+$ ion-beam profile overlapped the $^{17}O^+$ ion beam, some ^{16}O ($I = 0$) was also implanted which accounts for most of the fine-structure spectrum in Fig. 2.[5]

The EPR measurements were made with a K-band superheterodyne spectrometer. The EPR spectra were observed in the dispersion mode under the following typical conditions: $T_{\text{sample}} \simeq 15$ to 25 K, $P_{\text{microwave}} \simeq 4$ μW, $Q_{\text{loaded}} \simeq 5000$ (TE_{011}

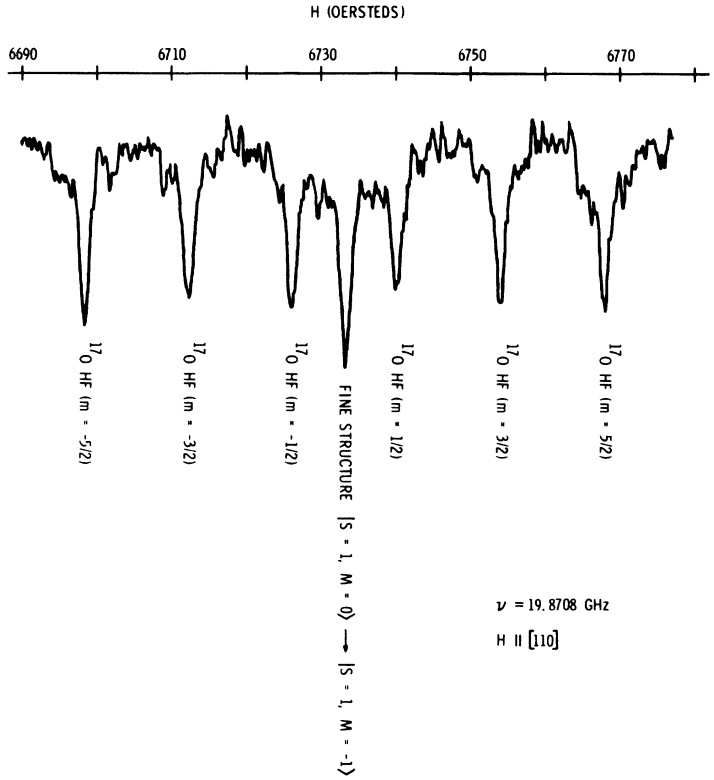

FIG. 2. EPR ^{17}O hyperfine and fine-structure spectra associated with the ^{28}Si-^{17}O-^{28}Si and ^{28}Si-^{16}O-^{28}Si isotopic configurations of the Si-$S1$ center, respectively. These spectra were observed in a sample of n-type vacuum-float-zone silicon implanted with 3×10^{14} $^{17}O^+/cm^2$ at 180 keV. As a result of populating the triplet spin levels of the Si-$S1$ center by light, a population inversion is achieved so that these particular resonances correspond to emission transitions.

cylindrical copper cavity), and $H_{p\text{-}to\text{-}p\ mod} \simeq 0.5$ Oe at ~100 Hz. Since the Si-*S*1 spectrum is observed only under illumination with approximately band-gap light,[1] the sample was illuminated by means of two subminiature lamps mounted in the wall of the cavity. The intensity of the Si-*S*1 spectrum associated with the implanted oxygen was weak to very weak. The signal to noise of the very weak spectra was enhanced by signal-averaging techniques.

III. ANALYSIS

A. Spin Hamiltonian

The general form of the spin Hamiltonian which describes the ^{17}O ($I = \frac{5}{2}$) hyperfine spectrum arising from the ^{28}Si-^{17}O-^{28}Si isotopic configuration of the Si-*S*1 center is

$$\mathcal{H} = \frac{1}{2} \begin{bmatrix} \vec{H} \\ \vec{S}_1 \\ \vec{S}_2 \\ \vec{I} \end{bmatrix}^{\dagger} \cdot \begin{bmatrix} 0 & \mu_B \vec{g}_1 & \mu_B \vec{g}_2 & \vec{\gamma} \\ \mu_B \vec{g}_1^{\dagger} & 0 & \vec{K} & \vec{A}_1 \\ \mu_B \vec{g}_2^{\dagger} & \vec{K}^{\dagger} & 0 & \vec{A}_2 \\ \vec{\gamma}^{\dagger} & \vec{A}_1^{\dagger} & \vec{A}_2^{\dagger} & 2\vec{Q} \end{bmatrix} \cdot \begin{bmatrix} \vec{H} \\ \vec{S}_1 \\ \vec{S}_2 \\ \vec{I} \end{bmatrix} . \tag{1}$$

In this spin Hamiltonian, $\vec{H}$ is the applied magnetic field, $\vec{S}_1$ and $\vec{S}_2$ are the electron spin operators, and $\vec{I}$ is the ^{17}O nuclear spin operator. The spin states are of the form $|S_1 = \frac{1}{2}, M_1; S_2 = \frac{1}{2}, M_2; I = \frac{5}{2}, m\rangle$. The coupling tensors, $\vec{g}_1$, $\vec{g}_2$, $\vec{\gamma}$, $\vec{K}$, $\vec{A}_1$, $\vec{A}_2$, and $\vec{Q}$, define the interaction between any pair of the vectors $\vec{H}$, $\vec{S}_1$, $\vec{S}_2$, and $\vec{I}$. The electronic Zeeman interaction corresponds to the terms $\mu_B \vec{H} \cdot \vec{g}_1 \cdot \vec{S}_1 + \mu_B \vec{H} \cdot \vec{g}_2 \cdot \vec{S}_2$, where μ_B is the Bohr magneton ($\mu_B = 4.6686 \times 10^{-5}$ cm^{-1}/Oe); the nuclear Zeeman interaction corresponds to the term $\vec{H} \cdot \vec{\gamma} \cdot \vec{I}$. The electronic spin-spin interaction, which has previously been shown to be dominated by the magnetic dipole-dipole interaction,[1] is specified by a term of the form $\vec{S}_1 \cdot \vec{K} \cdot \vec{S}_2$. It is customary to separate this interaction into its isotropic, traceless symmetric, and antisymmetric parts so that

$$\vec{S}_1 \cdot \vec{K} \cdot \vec{S}_2 = J \vec{S}_1 \cdot \vec{S}_2 + \vec{S}_1 \cdot \vec{D} \cdot \vec{S}_2 + \vec{S}_1 \cdot \vec{a} \cdot \vec{S}_2 , \tag{2}$$

where $\mathrm{Tr}(\vec{D}) = 0$. The ^{17}O hyperfine interaction, which is of prime interest in this study, corresponds to the terms $\vec{S}_1 \cdot \vec{A}_1 \cdot \vec{I} + \vec{S}_2 \cdot \vec{A}_2 \cdot \vec{I}$. Since $I = \frac{5}{2}$, there is also an electric quadrupole interaction which is specified by the term $\vec{I} \cdot \vec{Q} \cdot \vec{I}$ in Eq. (1).

The most general form for each of the coupling tensors belonging to the ^{28}Si-^{17}O-^{28}Si isotopic configuration of the Si-*S*1 center was derived following the group-theoretical method of Kneubühl.[6] The general form for each of these coupling tensors is tabulated in Table I. These coupling tensors are of such a form that nonzero matrix elements exist between the triplet and singlet states. Since the coupling between the singlet and triplet states of this defect has previously been shown to be negligible,[1] additional constraints on the coupling tensors can be introduced which reduce $\langle S_1 = \frac{1}{2}, M_1; S_2 = \frac{1}{2}, M_2; I = \frac{5}{2}, m | \mathcal{H} | S_1 = \frac{1}{2}, M_1'; S_2 = \frac{1}{2}, M_2'; I = \frac{5}{2}, m' \rangle$ to the pure triplet and singlet representations. The reduced forms of the coupling tensors which

TABLE I. Tabulation of the general forms of the coupling tensors belonging to the spin Hamiltonian in Eq. (1). For the ^{28}Si-^{17}O-^{28}Si isotopic configuration, the reduced coupling tensors correspond only to the diagonal elements of the general coupling tensors. The principal axes are defined in Fig. 1 with respect to the vacancy-oxygen center.

Tensors	^{17}O hyperfine spectrum ^{28}Si-^{17}O-^{28}Si configuration General form of coupling tensors
g_1	$\begin{pmatrix} g_{xx} & 0 & 0 \\ 0 & g_{yy} & g_{yz} \\ 0 & g_{zy} & g_{zz} \end{pmatrix}$
g_2	$\begin{pmatrix} g_{xx} & 0 & 0 \\ 0 & g_{yy} & -g_{yz} \\ 0 & -g_{zy} & g_{zz} \end{pmatrix}$
K	$\begin{pmatrix} K_{xx} & 0 & 0 \\ 0 & K_{yy} & K_{yz} \\ 0 & -K_{yz} & K_{zz} \end{pmatrix}$
γ	$\begin{pmatrix} \gamma_{xx} & 0 & 0 \\ 0 & \gamma_{yy} & 0 \\ 0 & 0 & \gamma_{zz} \end{pmatrix}$
Q	$\begin{pmatrix} Q_{xx} & 0 & 0 \\ 0 & Q_{yy} & 0 \\ 0 & 0 & Q_{zz} \end{pmatrix}$
A_1	$\begin{pmatrix} A_{xx} & 0 & 0 \\ 0 & A_{yy} & A_{yz} \\ 0 & A_{zy} & A_{zz} \end{pmatrix}$
A_2	$\begin{pmatrix} A_{xx} & 0 & 0 \\ 0 & A_{yy} & -A_{yz} \\ 0 & -A_{zy} & A_{zz} \end{pmatrix}$

TABLE II. Tabulation of the $\overleftrightarrow{g}$, $\overleftrightarrow{D}$, and $\overleftrightarrow{A}$ tensors associated with the ^{28}Si-^{17}O-^{28}Si isotopic configuration of the Si-$S1$ center. The principal axes for these coupling tensors are defined with respect to the defect in Fig. 1.

	g tensor[1] ± 0.0001		D tensor[1] (in units of 10^{-4} cm^{-1}) ± 0.1			^{17}O hyperfine tensor (in units of 10^{-4} cm^{-1}) ± 0.3		
g_{xx}	g_{yy}	g_{zz}	D_{xx}	D_{yy}	D_{zz}	A_{xx}	A_{yy}	A_{zz}
2.0102_0	2.0057_6	2.0075_7	204.8_0	-438.3_1	233.5_1	-11.5_1	-12.9_0	-13.3_9

accomplish this correspond only to the diagonal elements of the general coupling tensors tabulated in Table I.

B. Numerical Analysis and Results

From the analysis of the EPR spectrum arising from the ^{28}Si-^{16}O-^{28}Si isotopic configuration of the Si-$S1$ center, the numerical values for the $\overleftrightarrow{g}_1$, $\overleftrightarrow{g}_2$, and $\overleftrightarrow{D}$ coupling tensors have been determined previously.[1] Consequently only the numerical values for the $\overleftrightarrow{A}_1$, $\overleftrightarrow{A}_2$, $\overleftrightarrow{\gamma}$, and $\overleftrightarrow{Q}$ coupling tensors in Eq. (1) associated with the ^{17}O atom in the Si-$S1$ center need to be determined.

The $\overleftrightarrow{A}_1$, $\overleftrightarrow{A}_2$, $\overleftrightarrow{\gamma}$, and $\overleftrightarrow{Q}$ reduced coupling tensors are characterized by nine independent parameters. The electric quadrupole interaction which is specified by the $\overleftrightarrow{Q}$ tensor is expected to be small ($\sim 10^{-6}$ cm^{-1}) compared with the nuclear Zeeman interaction ($\sim 10^{-4}$ cm^{-1}). Because the electric quadrupole interaction is very weak, it has no perceptible effect on the position of the EPR lines in the ^{17}O hyperfine spectrum.[7] Since we are unable to deduce the numerical values for the $\overleftrightarrow{Q}$ tensor from our EPR spectra, the $\overleftrightarrow{Q}$ tensor is excluded from further consideration in this paper.

Although the nuclear Zeeman interaction is small ($\sim 10^{-4}$ cm^{-1}), it does have a perceptible effect on the position of the EPR lines in the ^{17}O hyperfine spectrum. The splittings between the energy levels corresponding to the $|S = 1, M = 0; I, m\rangle$ states arise in zeroth order from the nuclear Zeeman interaction and in second order from the ^{17}O hyperfine and electronic spin-spin interactions. Furthermore, the perturbation on these levels due to the nuclear Zeeman interaction is comparable to the perturbation in these levels which occurs if the sign of the $\overleftrightarrow{A}_1$ and $\overleftrightarrow{A}_2$ tensors is changed. Consequently, one can only be assured of deducing the correct signs for the $\overleftrightarrow{A}_1$ and $\overleftrightarrow{A}_2$ tensors providing the nuclear Zeeman interaction is retained. Because the nuclear Zeeman interaction is weak and is expected to experience practically no interaction with the silicon lattice, the $\overleftrightarrow{\gamma}$ tensor is taken to be isotropic and equal to $-\mu_n/I$, where $\mu_n = -1.8930$ μ_N[8] for ^{17}O ($\mu_N = 2.5427 \times 10^{-8}$ cm^{-1}/Oe).

Only three independent parameters which are contained within the $\overleftrightarrow{A}_1$ and $\overleftrightarrow{A}_2$ reduced coupling tensors need to be determined. The numerical values for the $\overleftrightarrow{A}_1$ and $\overleftrightarrow{A}_2$ reduced coupling tensors were determined by minimizing

$$\sum_i [\nu_{i,\text{expt}} - \nu_{i,\text{calc}}(H_{i,\text{expt}}, \theta_i, \overleftrightarrow{g}, \overleftrightarrow{D}, \overleftrightarrow{A}_1, \overleftrightarrow{A}_2, \gamma)]^2$$

as a function of these three independent parameters by a direct-search minimization procedure. This analysis was carried out on 36 allowed ^{17}O hyperfine transitions for $\vec{H}$ parallel to the [001], [110], and [1$\bar{1}$0] directions. For positive $\overleftrightarrow{A}_1$ and $\overleftrightarrow{A}_2$, the standard deviation in the least-squares fit was 1.37×10^{-2} GHz (~ 4.9 Oe), whereas the standard deviation in the least-squares fit for negative $\overleftrightarrow{A}_1$ and $\overleftrightarrow{A}_2$ was 8.35×10^{-4} GHz (~ 0.3 Oe). Since the accuracy with which we can measure the absolute magnetic field position of our resonances is ±0.3 Oe, this analysis indicates that the sign of the $\overleftrightarrow{A}_1$ and $\overleftrightarrow{A}_2$ tensors is negative. The negative sign of the $\overleftrightarrow{A}_1$ and $\overleftrightarrow{A}_2$ tensors is also consistent with the signs predicted by the hyperfine interaction (see Sec. III D). The numerical results of this analysis are tabulated in Table II.

C. Electronic Structure

If the oxygen atom were at the origin of the xyz coordinate system in Fig. 1, then the vacancy-oxygen center would have T_d symmetry. The irreducible representations within the group T_d to which the $\psi_{2s,0}$, $\psi_{2p_x,0}$, $\psi_{2p_y,0}$, and $\psi_{2p_z,0}$ orbitals localized on the oxygen atom and the various silicon ligands, $\varphi_l (l = 1, 2, 3, 4)$, belong are tabulated in Table III. Although the order and energy splittings between these levels are unknown, one might expect a relatively large energy gap between the bonding levels (Γ_1' and Γ_5) and the antibonding levels ($\Gamma_1'^*$ and Γ_5^*). Furthermore, a Γ_1 state is usually the lowest energy level of an atomic system. A plausible energy-level diagram for the vacancy-oxygen center having T_d symmetry is illustrated in Fig. 3.

In the neutral charge state, the energy-level diagram in Fig. 3 is occupied by 10 electrons. If the Γ_5^* is only partially filled, then according to the Jahn-Teller theorem the vacancy-oxygen center will be distorted from T_d symmetry to a lower symmetry and energy, thereby removing the degeneracy of the Γ_5 levels. The fact that the vacancy-oxygen center has C_{2v} symmetry[1] rather than T_d symmetry is consistent with the idea[4] that the

TABLE III. Classification of the oxygen-valence orbitals and the silicon hybrid orbitals within the vacancy-oxygen defect having (hypothetical) T_d and (actual) C_{2v} symmetry. The x, y, z directions are defined with respect to the crystallographic directions in Fig. 1.

Symmetry	Irreducible representation	Oxygen orbitals	Silicon ligands
T_d	Γ_1	$\psi_{2s,0}$	$\varphi_1+\varphi_2+\varphi_3+\varphi_4$
	Γ_5	$\psi_{2p_x,0}$	$\varphi_1-\varphi_2$
		$\psi_{2p_y,0}$	$\varphi_3-\varphi_4$
		$\psi_{2p_z,0}$	$\varphi_1+\varphi_2-\varphi_3-\varphi_4$
C_{2v}	Γ_1	$\psi_{2s,0}$	$\varphi_1+\varphi_2$
		$\psi_{2p_z,0}$	$\varphi_3+\varphi_4$
	Γ_2	$\psi_{2p_x,0}$	$\varphi_1-\varphi_2$
	Γ_4	$\psi_{2p_y,0}$	$\varphi_3-\varphi_4$

oxygen atom is displaced along the z axis from the normal silicon lattice site as illustrated in Fig. 1. The fact that the vacancy-oxygen center reorients spontaneously for temperatures $\gtrsim 135$ K[1,4] suggests that the splittings between levels originating from within the Γ_5 manifold may tend to be comparatively small. Although the exact energy-level splittings and the details concerning the order of these levels are not yet known, some of the more general aspects of the electronic structure of the vacancy-oxygen center are illustrated in Fig. 3.

D. ^{17}O Hyperfine Interaction

The silicon ligand φ_l localized on the lth silicon atom ($l=1, 2, 3, 4$) in Fig. 1 can be expressed in terms of normalized $3s$, $3p$ hybrid orbitals of the form

$$\varphi_l=\alpha_l\psi_{3s,l}+\beta_l\psi_{3p,l}\ , \tag{3}$$

where α_l and β_l are parameters which define the admixture of $3s$ and $3p$ orbitals at the lth silicon sites. The irreducible representations within the group C_{2v} to which the $\psi_{2s,0}$, $\psi_{2p_x,0}$, $\psi_{2p_y,0}$, and $\psi_{2p_z,0}$ orbitals localized on the oxygen atom and the various silicon ligands φ_l belong are tabulated in Table III.

A previous analysis[1] of the ^{29}Si hyperfine interactions indicates that the two paramagnetic electrons are mostly localized on a pair of silicon atoms in the same (110) plane. For definiteness, we choose these to be atoms 3 and 4 in Fig. 1. Table III indicates that one-electron molecular orbitals which transform as Γ_1 and Γ_4 can have significant admixtures of φ_3 and φ_4. The one-electron molecular orbitals which transform as Γ_1 and Γ_4 can be expressed as

$$\chi_1=\eta_{1,0}(\alpha_0\psi_{2s,0}+\beta_0\psi_{2p_z,0})+\eta_{1,3}(\varphi_3+\varphi_4)+\cdots \tag{4}$$

and

$$\chi_4=\eta_{4,0}\psi_{2p_y,0}+\eta_{4,3}(\varphi_3-\varphi_4)+\cdots\ , \tag{5}$$

respectively.[9] The parameters $\eta_{k,l}$ specify the admixture of various hybrid orbitals belonging to the Γ_k representation at the lth site. This choice of one-electron molecular orbitals is also consistent with the isotropic character of the ^{17}O hyperfine interaction (see Table II) which suggests that one of the χ's is partially s-like. Consequently, the antisymmetric combination of one-electron molecular orbitals which describes the paramagnetic electrons in the excited triplet spin state is of the form

$$\Psi(\vec{x}_1,\vec{x}_2)=[\chi_1(\vec{x}_1)\chi_4(\vec{x}_2)-\chi_1(\vec{x}_2)\chi_4(\vec{x}_1)]/\sqrt{2}\ . \tag{6}$$

The hyperfine interaction which describes the magnetic interaction between two electrons and a nucleus is

$$\mathcal{H}_{\rm HF}=\frac{16\pi}{3}\mu_B\frac{\mu_n}{I}\sum_{k=1}^{2}\delta(\vec{r}_k)\vec{S}_k\cdot\vec{I}$$
$$-2\mu_B\frac{\mu_n}{I}\sum_{k=1}^{2}\left(\frac{\vec{S}_k\cdot\vec{I}}{r_k^3}-\frac{3(\vec{S}_k\cdot\vec{r}_k)(\vec{I}_k\cdot\vec{r}_k)}{r_k^5}\right)$$

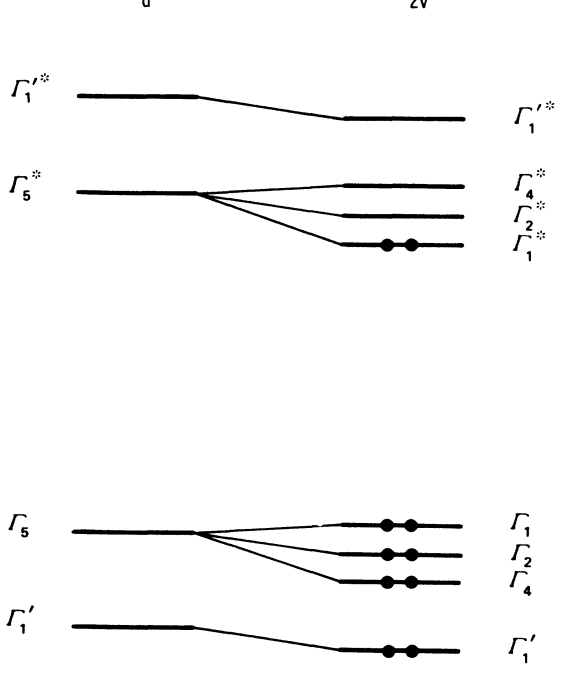

FIG. 3. Possible energy-level diagram of the neutral vacancy-oxygen center in the diamagnetic ($S=0$) ground state. In this energy-level diagram, a Jahn-Teller distortion lowers the symmetry of the defect from T_d to C_{2v} and lifts the degeneracy of the Γ_5 levels.

$$+ 2\mu_B \frac{\mu_n}{I} \sum_{k=1}^{2} \frac{\vec{L}_k \cdot \vec{I}}{r_k^3} \quad . \tag{7}$$

In this expression, $\vec{I}$, $\vec{S}_k$, and $\vec{L}_k$ are the actual nuclear-spin, electron-spin, and orbital-angular-momentum operators; $\vec{r}_k$ is the distance between the kth electron and the nucleus.

To a first approximation, the relationship between the ^{17}O hyperfine coupling tensors, $\overleftrightarrow{A}_1$ and $\overleftrightarrow{A}_2$, and the parameters α_0^2, β_0^2, $\eta_{1,0}^2$, and $\eta_{4,0}^2$ in χ_1 and χ_4 [see Eqs. (4) and (5)] can be determined. In developing this relationship, one notes that the orbital angular momentum of the Si-$S1$ center is very nearly quenched (as evidenced by the value of the Si-$S1$ $\overleftrightarrow{g}$ tensor which is very nearly equal to that of a free electron). Consequently, the contribution to the ^{17}O hyperfine interaction arising from the third term in Eq. (7), which accounts for the magnetic interaction between the electronic orbital and nuclear magnetic moments, can be neglected. Under these circumstances, the nuclear and electron-spin operators in Eq. (7) correspond directly to those in Eq. (1). In order to evaluate the matrix element $\langle \Psi(\vec{x}_1, \vec{x}_2) | \mathcal{H}_{HF} \times | \Psi(\vec{x}_1, \vec{x}_2) \rangle$ explicitly, we have neglected the contributions in χ_1 and χ_4 arising from the silicon ligands. As a result of these approximations, the relationship between the parameters in the one-electron molecular orbitals and the $\overleftrightarrow{A}_1$ and $\overleftrightarrow{A}_2$ coupling tensors are given to a first approximation by the expressions

$$A_{1xx} = A_{2xx} = \frac{8\pi}{3} \mu_B \frac{\mu_n}{I} \eta_{1,0}^2 \alpha_0^2 |\psi_{2s,0}(0)|^2 + \mu_B \frac{\mu_n}{I} \left(\frac{-2\eta_{1,0}^2 \beta_0^2 - 2\eta_{4,0}^2}{5} \right) \langle r_{2p}^{-3} \rangle , \tag{8}$$

$$A_{1yy} = A_{2yy} = \frac{8\pi}{3} \mu_B \frac{\mu_n}{I} \eta_{1,0}^2 \alpha_0^2 |\psi_{2s,0}(0)|^2 + \mu_B \frac{\mu_n}{I} \left(\frac{-2\eta_{1,0}^2 \beta_0^2 + 4\eta_{4,0}^2}{5} \right) \langle r_{2p}^{-3} \rangle , \tag{9}$$

and

$$A_{1zz} = A_{2zz} = \frac{8\pi}{3} \mu_B \frac{\mu_n}{I} \eta_{1,0}^2 \alpha_0^2 |\psi_{2s,0}(0)|^2 + \mu_B \frac{\mu_n}{I} \left(\frac{4\eta_{1,0}^2 \beta_0^2 - 2\eta_{4,0}^2}{5} \right) \langle r_{2p}^{-3} \rangle . \tag{10}$$

The first term in Eqs. (8)–(10) arises from the Fermi contact interaction and contributes to the isotropic part of the $\overleftrightarrow{A}_1$ and $\overleftrightarrow{A}_2$ tensors [$\mathrm{Tr}(\overleftrightarrow{A}_1) = \mathrm{Tr}(\overleftrightarrow{A}_2) = 8\pi\mu_B(\mu_n/I)\eta_{1,0}^2\alpha_0^2|\psi_{2s,0}(0)|^2$]. The second term in Eqs. (8)–(10) arises from the magnetic dipole-dipole interaction between the paramagnetic electrons and the ^{17}O nucleus. The second term in Eqs. (8)–(10) contributes only to the anisotropy in the $\overleftrightarrow{A}_1$ and $\overleftrightarrow{A}_2$ tensors. Since the $\overleftrightarrow{A}_1$ and $\overleftrightarrow{A}_2$ coupling tensors are observed to be nearly isotropic (see Table II), the ^{17}O hyperfine interaction is dominated by the Fermi contact interaction. Consequently, the $\overleftrightarrow{A}_1$ and $\overleftrightarrow{A}_2$ tensors are expected to be negative since $\mu_n = -1.8930\ \mu_N$, and all of the other parameters in the Fermi contact term are positive definite.

Before these equations can be solved, $|\psi_{2s,0}(0)|^2$ and $\langle r_{2p}^{-3} \rangle$ need to be specified. The Hartree-Fock wave functions for the ground ^3P multiplet of free oxygen as calculated by Mann[10] indicate that $|\psi_{2s}(0)|^2 = 51.60 \times 10^{24}$ cm^{-3}. The EPR measurements of Harvey[11] on the ^3P multiplet of free ^{17}O indicate that $\langle r_s^{-3} \rangle$ associated with the dipole-dipole term is equal to 35.03×10^{24} cm^{-3}.

Using the values of Mann and Harvey for $|\psi_{2s,0}(0)|^2$ and $\langle r_{2p}^{-3} \rangle$, respectively, the numerical values for α_0^2, β_0^2, $\eta_{1,0}^2$, and $\eta_{4,0}^2$, which characterize the admixture of the oxygen ψ_{2s}, ψ_{2p_z}, and ψ_{2p_y} orbitals into χ_1 and χ_4, can be deduced and are tabulated in Table IV. In this analysis, the contributions arising from cross terms of the form $\eta_{1,0}\eta_{1l}|\psi_{2s,0}(0)\,\varphi_l(0)|$ and $\eta_{1l}\eta_{1m}|\varphi_l(0)\,\varphi_m(0)|$ to the Fermi contact hyperfine interaction have been neglected. Although terms of the form $\eta_{1l}\eta_{1m}|\varphi_l(0)\,\varphi_m(0)|$ are negligible, the cross terms $\eta_{1,0}\eta_{1l}|\psi_{2s,0}(0)\varphi_l(0)|$ contribute ~10% to the trace of $\overleftrightarrow{A}_1$ and $\overleftrightarrow{A}_2$. Although it is difficult to estimate the contributions to the anisotropy in $\overleftrightarrow{A}_1$ and $\overleftrightarrow{A}_2$ arising from similar cross terms with the dipole-dipole interaction, the results of Zeller and Känzig[12] indicate that $\langle r_s^{-3} \rangle$ increases by ~8% in going from free oxygen to O_2^- in the alkali halides. These factors alone impose uncertainties in α_l^2, β_l^2, $\eta_{1,0}^2$, and $\eta_{4,0}^2$ of ~10%. The previously determined[1] values of α_l^2, β_l^2, and $\eta_{1l}^2 + \eta_{4l}^2$ which pertain to the character of the wave function at silicon sites 3 and 4 are also tabulated in Table IV.

IV. DISCUSSION AND CONCLUSIONS

In silicon containing the natural abundance of oxygen isotopes, the intensity of the Si-$S1$ ^{17}O hyperfine spectrum relative to the fine-structure spectrum is 3.7×10^{-4}. Under these circumstances, the ^{17}O hyperfine spectrum is buried in the spectra

TABLE IV. Character of the wave function as deduced from the ^{17}O and ^{29}Si (Ref. 1) hyperfine interactions.

Site	α_l^2	β_l^2	$\eta_{1,0}^2$	$\eta_{4,0}^2$	$\eta_{1,l}^2 + \eta_{4,l}^2$
oxygen ($l=0$)	0.40	0.60	0.041	0.018	···
silicon ($l=1, 2$)	0.12	0.88	···	···	0.64

arising from the other more abundant isotopic configurations of the Si-S1 center. Using the technique of ion implantation, we have been able to enhance the concentration of ^{17}O in our samples so that the intensity of the ^{17}O hyperfine spectrum relative to the fine-structure spectrum is observed to be 4.3 (see Fig. 2).

The ability to dope a crystal with a particular impurity and isotope offers distinct advantages to many spin-resonance studies. Part of the significance of this study is that EPR measurements were made on a sample doped by ion implantation. This is significant not only because it is possible to enhance the concentration of a rare isotope as demonstrated here, but also because ion implantation is a nonthermal equilibrium process. Consequently, the doping of a crystal with a particular impurity and isotope by ion implantation tends to be limited by technological techniques rather than by thermal-equilibrium processes. Furthermore, the efficiency for incorporating into a sample an isotope, which is usually available only in limited quantities and chemical forms, is very high by ion implantation.

From an analysis of the Si-S1 ^{17}O hyperfine spectrum, the numerical values for the reduced coupling tensors $\overleftrightarrow{A}_1$ and $\overleftrightarrow{A}_2$ in the spin Hamiltonian of Eq. (1) were determined. The numerical values for $\overleftrightarrow{A}_1$ and $\overleftrightarrow{A}_2$ as well as the other coupling tensors are tabulated in Table II (see also Sec. III B).

From group theory, the proper linear combinations of oxygen-valence orbitals and silicon ligands compatible with the C_{2v} symmetry of the Si-S1 center can be determined. From the basis functions tabulated in Table III, eight linearly independent molecular orbitals can be constructed. In general, these molecular orbitals tend to be localized on a Si-O-Si complex lying in either the (110) or (1$\bar{1}$0) plane in Fig. 1. The two molecular orbitals which we were able to examine by virtue of the spin resonance arising from the unpaired electrons in these molecular orbitals are situated in the same plane and are of the form of Eqs. (4) and (5).

The results of our analysis tabulated in Table IV indicate that only 4.0% of $\langle\chi_1|\chi_1\rangle$ and 1.8% of $\langle\chi_4|\chi_4\rangle$ are localized on the oxygen atom. On the other hand, 64% of $\langle\chi_1|\chi_1\rangle + \langle\chi_4|\chi_4\rangle$ is localized at each of the silicon sites 3 and 4 in Fig. 1. The next-nearest-neighbor ^{29}Si hyperfine spectrum[1] indicates that $\lesssim 2\%$ of $\langle\chi_1|\chi_1\rangle + \langle\chi_4|\chi_4\rangle$ is localized at any one site neighboring this Si-O-Si complex. From Table IV, the s and p character of the oxygen hybrid orbital φ_0 contained within χ_1 can be specified; 40% of $\langle\varphi_0|\varphi_0\rangle$ arises from ψ_{2s}, and 60% of $\langle\varphi_0|\varphi_0\rangle$ arises from ψ_{2p_z}. As indicated in Sec. III D, the isotropic part of the hyperfine interaction originates from the s-like part of the wave function, while the anisotropic contribution to the corresponding hyperfine interaction reflects the non-s-state character of the wave function.

Very few fundamental theoretical studies of the electronic structure have been done for radiation-induced defects in silicon. The relative simplicity of the vacancy-oxygen center and the wealth of experimental data relating to its electronic and molecular structure appear to make this an attractive defect on which to perform a first-principles theoretical analysis.

ACKNOWLEDGMENTS

It is a pleasure to acknowledge the assistance of N. D. Wing who made the EPR measurements and A. G. Bromberg who assisted us with the ion implants. The author has also benefited from discussions with D. K. Brice and F. L. Vook concerning various aspects of this work.

---

†Work supported by the U. S. Atomic Energy Commission.

[1]K. L. Brower, Phys. Rev. B 4, 1968 (1971).

[2]G. Bemski, J. Appl. Phys. 30, 1195 (1959).

[3]G. D. Watkins, J. W. Corbett, and R. M. Walker, J. Appl. Phys. 30, 1198 (1959).

[4]G. D. Watkins and J. W. Corbett, Phys. Rev. 121, 1001 (1961).

[5]Although this is the dominant source of ^{16}O which gives rise to the fine structure spectrum, it is not the only source. We have observed that after ion implantation with only $^4He^+$ or $^{20}Ne^+$, a Si-S1 fine structure spectrum $\sim\frac{1}{4}$ as intense as that in Fig. 2 is usually observed.

[6]F. K. Kneubühl, Physik Kondensierten Materie 1, 410 (1963).

[7]In general, an EPR line is shifted $\lesssim N$ Oe due to an interaction whose energy is $N\times 10^{-4}$ cm^{-1}. Since the resonances in the Si-S1 spectrum have a full width of ~ 1.5 Oe at half-maximum, the effects of the quadrupole interaction ($\sim 10^{-6}$ cm^{-1}) are unresolved.

[8]Varian Associates, NMR Table, 4th ed., 1964 (unpublished).

[9]To be definite, we have chosen to have φ_3 and φ_4 as the silicon ligands in the wave function. The analysis which follows would be exactly the same if φ_1 and φ_2 had been chosen except that χ_4 would be replaced by χ_2, ψ_{2p_y} by ψ_{2p_x}, and φ_3 and φ_4 by φ_1 and φ_2. The admixture of silicon orbitals on other silicon sites in Eqs. (4) and (5) is acknowledged but does not need to be specified for the purposes of this study.

[10]J. B. Mann (unpublished).

[11]J. S. M. Harvey, Proc. Roy. Soc. (London) A285, 581 (1965).

[12]H. R. Zeller and W. Känzig, Helv. Phys. Acta 40, 845 (1967).

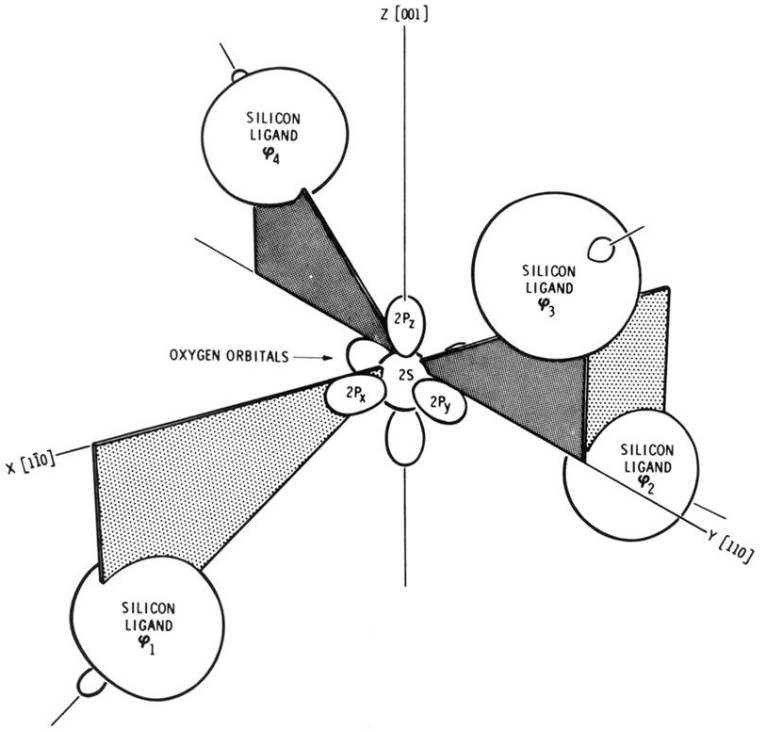

FIG. 1. Structure of the vacancy-oxygen center in silicon. In this schematic, the oxygen atom is displaced along the z axis from the tetrahedral site (origin of XYZ). This distortion lowers the symmetry of the defect from T_d to C_{2v}. The allowed linear combinations of silicon ligands φ_i and oxygen orbitals for these symmetries are tabulated in Table III.